Journal of Renewable Materials

Tech Science Press

DOI: 10.32604/jrm.2024.056334

ARTICLE

Characterization and Performance Evaluation of Mycelium-Based Biofoams for Cushioning Materials Using Edible Mushrooms

Tanyawan Suwandecha[1] and Supachai Pisuchpen[2,*]

[1]Program of Food Packaging Technology, Faculty of Agro-Industry, Prince of Songkla University, Hat Yai Campus, Songkhla, 90110, Thailand

[2]Center of Excellence in Bio-Based Materials and Packaging Innovation, Faculty of Agro-Industry, Prince of Songkla University, Hat Yai Campus, Songkhla, 90110, Thailand

[*]Corresponding Author: Supachai Pisuchpen. Email: supachai.p@psu.ac.th

Received: 20 July 2024 Accepted: 21 August 2024 Published: 22 November 2024

ABSTRACT

This study investigated the development of mycelium-based biofoams as sustainable cushioning materials using *Pleurotus ostreatus* and *Lentinus squarrosulus*, combined with different sawdust substrates, and subjected to various pressing methods. The results indicated significant effects of mushroom species, sawdust type, and pressing method on the properties of biofoams. Growth rate, morphology, chemical composition, physical and mechanical properties, water resistance, and cushioning factor were evaluated. The results indicated that *Lentinus squarrosulus* (LS) exhibited faster growth rates (up to 14.37 mm/day) and produced biofoams with superior properties compared to *Pleurotus ostreatus* (PO). Core wood (CW) sawdust generally resulted in biofoams with lower density (0.1–0.3 g/cm^3), lower shrinkage (7.17%–11.41%), and better shock absorption properties (cushion factor of 4.45–4.73). Hot pressing (HO) consistently produced biofoams with higher density (up to 0.31 g/cm^3), improved mechanical strength (compression strength up to 0.53 MPa), and enhanced hydrophobicity (water contact angle up to 102.03°) but slightly reduced the shock absorption performance. Biofoam made from LS cultivated on CW sawdust and pressed using hand-packing (HP) exhibited superior shock absorption properties, achieving a cushion factor of 4.45 comparable to expanded polystyrene (EPS) foam. The findings demonstrated that certain combinations of sawdust types and pressing methods can optimize the performance of mycelium-based biofoams, making them viable for sustainable packaging applications. This study highlighted the potential of mycelium biofoams as an eco-friendly alternative to conventional packaging materials, thereby decreasing environmental impact and promoting a sustainable future.

KEYWORDS

Mycelium; *Pleurotus ostreatus*; *Lentinus squarrosulus*; cushioning materials; cushion factor; packaging

1 Introduction

The protection of products is always the top focus, and packaging plays the most important role in ensuring that all products reach their destination without damage. Cushioning packaging is the most popular method to protect products by absorbing the mechanical energy generated by shock and vibration. However, the ability of energy absorption depends on cushioning properties, shape, size, and materials. Polystyrene is widely used in cushioning packaging because of its low cost, light weight,

and ability to absorb shock. Despite its numerous advantages, it still affects the environment. Polystyrene is non-biodegradable, meaning that it lingers for hundreds of years, causing long-term waste issues. It breaks down into microplastics that pollute water, harm marine life, and contribute to climate change. The need for sustainable, recyclable, and biodegradable alternatives has driven research on bio-based materials. Mycelium-based biofoams have gained attention for their outstanding physical and mechanical properties in various applications, particularly as ecofriendly protective packaging materials. The mycelium, the vegetative part of a fungus, forms an interwoven network of hyphae that can absorb and distribute shocks, making it suitable for cushioning applications. The combination of mycelium with agricultural or industrial residues to create biofoams presents a novel approach that addresses both environmental and performance concerns. Mycelium-based biofoams are prepared by initially cultivating pure mycelium on a media culture, which is then inoculated into a sterilized substrate. The inoculated substrate is packed into a sterilized mold and allowed to grow in a controlled environment to form the desired shape. After sufficient growth, the biofoam is hot air-dried to stop further growth and dry it (Fig. 1).

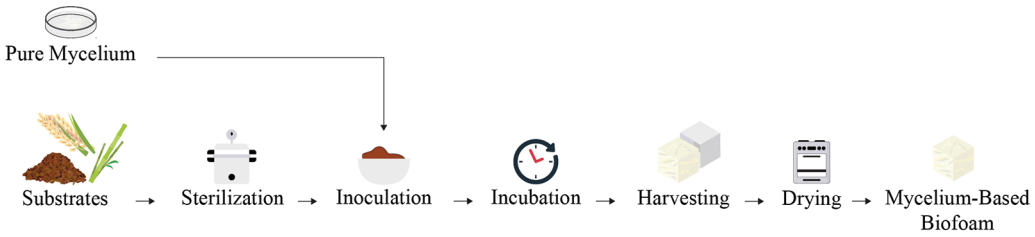

Figure 1: General preparation process of mycelium-based biofoams

Previous studies have reported the potential of mycelium-based biofoams, highlighting their low density, low energy consumption, and performance characteristics, similar to those of polystyrene [1–4]. Despite the potential of mycelium-based biofoams, there are noticeable gaps in existing research. Previous studies have largely focused on the basic properties and performance of mycelium biofoams, but interesting aspects, such as the impact of density, methods to control or achieve uniform density, and comprehensive evaluations of cushioning performance, remain underexplored. Understanding how to control and achieve uniform density is crucial, as it directly influences the material's ability to absorb and dissipate energy during impact; however, while some studies have been conducted on the cushioning performance of mycelium-based biofoams, there is a lack of comprehensive studies evaluating their cushion performance via the cushion factor and cushion curve, which are fundamental parameters for packaging design in protective packaging and are essential for comparing the performance of mycelium-based biofoams with conventional materials such as EPS foam. Addressing these research gaps is crucial for advancing mycelium-based biofoams for their widespread adoption as sustainable packaging materials. This ongoing research attempts to pave the way for these biofoams to be a fresh and eco-friendly option for businesses and industries that aim to strike a balance between protective packaging and environmental responsibility.

This study was conducted to bridge essential knowledge gaps by examining mycelium-based biofoams derived from two edible mushrooms, *Pleurotus ostreatus* and *Lentinus squarrosulus*, which are economically significant in Thailand. These mushrooms can thrive on various substrates and adapt growth, according to environmental conditions. These are combined with wood sawdust, a by-product of the rubberwood industry in the southern region, which includes three types of wood sawdust: general or commercial, surface, and core sawdust. However, it is essential to note that the properties of mycelium-based

biofoams are influenced by several factors. This study focuses on evaluating the effects of different sawdust types, culture media, and pressing methods on the growth rate, morphology, chemical composition, physical and mechanical properties, water resistance, and cushioning performance of biofoams. By providing fundamental information on these biofoams, this study aims to motivate further development of sustainable packaging solutions. The integration of mycelium-based biofoams into packaging not only offers an innovative approach to reducing environmental impact, but also aligns with the principles of the Bio-Circular-Green Economy (BCG Economy), promoting sustainable development and economic growth in the global society.

2 Materials and Methods

2.1 Materials

Mycelium cultures of *Pleurotus ostreatus* (PO) and *Lentinus squarrosulus* (LS) were acquired from a mushroom farm in Thailand and prepared as dikaryotic cultures on agar. Potato Dextrose Agar (PDA) and Yeast extract powder, sourced from Himedia, India, were utilized in the study, with other chemicals procured from Ajax Finchem, Australia. Bran and millet grains were purchased from the local market in Songkla, Thailand. Rubberwood sawdust used in this study, general or commercial wood sawdust (CC), was purchased from a local store. The other two types of sawdust, surface wood sawdust (SW) and core wood sawdust (CW), were obtained from a local particleboard manufacturing factory. All types of rubberwood sawdust were cleaned to eliminate dirt, dust, and soil particles by soaking in tap water twice. Next, the wet sawdust was drained using a basket and subsequently rinsed with running water to remove residual dirt. It was then drained for 1 h in a basket. The wet sawdust was spread evenly in trays and dried in a hot-air oven at 70°C for 3 h. Finally, the dried sawdust was sieved to designated particle sizes ranging from 1 to 2 mm for commercial and surface wood sawdust, and 2 to 3 mm for core wood sawdust. The dried sawdust was stored in a laminated aluminum foil bag for the study.

2.2 Preparation of Pure Mycelium

To obtain pure mycelium, small pieces of *P. ostreatus* and *L. squarrosulus* were cultivated on PDA and incubated at 30°C, relative humidity (RH) of 70% for 5 days. Pure mycelium cultures of each species were isolated by transferring them to PDA as subcultures using a sterile cork borer.

2.3 Preparation of Rubberwood Sawdust Culture Media

Two culture media formulas were used as described by Krupadi et al. [5] and Werghemmi et al. [6]. The bran formula was prepared using 5% bran, 1% $CaCO_3$, 2% $CaSO_4$, and 0.2% $NaSO_4$. Dextrose formula consisted of 1% dextrose, 1.5% yeast extract powder, 2% $CaCO_3$, and 4% $CaSO_4$. The moisture content of the mixtures was adjusted to 70% by adding water. A 30 g sample of each formula was placed in a Petri dish. The dishes were then autoclaved at 121°C for 20 min.

2.4 Evaluation of Mycelium Growth Rate

2.4.1 Mycelium Cultivation

After cooling, a piece of pure mycelium with a diameter of 5 mm from each mushroom species was placed in the center of the previously prepared dishes in Section 2.3. Control dishes containing only wood sawdust without the addition of nutrients were included. All samples were incubated at 30°C, RH 70%.

2.4.2 Mycelium Growth Rate Measurements

Colony diameters or mycelium growth diameters (MGD) were measured daily until the mycelium completely covered all Petri dishes. Then, the mycelial linear growth rate (MLGR) was calculated using Eq. (1) [6,7].

$$\mathrm{MLGR}\left(\frac{\mathrm{mm}}{\mathrm{day}}\right) = \frac{\sum(\text{Diameter n}' - \text{Diameter n})}{\text{Incubation time}} \quad (1)$$

where MLGR (mm/day) is the mycelium linear growth rate, diameter n′ (mm) is the average diameter of the day, and diameter n (mm) is the average diameter of the previous day.

2.5 Preparation of Mycelium-Based Biofoams

2.5.1 Mycelium Inoculum Preparation

Each mushroom species was prepared using millet grain technique. The millet grains were cleaned by immersing them in water overnight to remove dust and soil, followed by boiling or steaming before drying. The dried grains were then transferred into ¾ glass bottles plugged with cotton wool and sterilized at 121°C for 20 min. Five small plugs (1 cm × 1 cm) of pure mycelium from each mushroom were inoculated into millet grains. All glass bottles were incubated at 30°C, RH 70% until the grains were observed with a bunch of mycelium fibers in the bottles.

2.5.2 Spawn Preparation

Each spawn was composed of different types of rubberwood sawdust and supplemented with the selected formula that most influenced growth rate, as determined in Section 2.4. The moisture content of all substrate mixtures was adjusted to 70% by adding water in polypropylene plastic bags. The substrates were then autoclaved at 121°C for 20 min. After cooling to room temperature, each sterilized bio-substrate was mixed with mycelium inoculum at a ratio of 1 part inoculum to 20 parts substrates (w/w). All bag samples were sealed with cotton to allow airflow, tied with a rubber band, and then incubated at 30°C, RH 70% for 5 days or until mycelium filaments were observed.

2.5.3 Mycelium-Based Biofoams Fabrication

Mycelium-based biofoams were fabricated using three methods: hand-packing (HP) and pressing machine: cold pressing (CO) and hot pressing (HO). Each spawn was hand-packed into square-shaped (50 mm × 50 mm × 25 mm) and rectangular molds for flexural strength testing (150 mm × 35 mm × 15 mm) using an aseptic technique.

a. For hand-packing method (HP), each spawn was hand-packed into a designated mold. The packed samples were then incubated under specific environmental conditions for 7 days. Afterwards, the samples were flipped over for an additional 3 days to allow for homogeneous colonization, and then demolded. Next, the samples were dried to halt further growth after demolding at 70°C for 24 to 72 h until their weight stabilized [8].

b. For the pressing method by machine: cold pressing (CO) and hot pressing (HO), samples were primarily prepared using from Section a, and then after demolding, the samples were first pre-compressed using a pressing machine for 1 min without heating to compact the sample. Next, the sample in the mold was topped by adding spawn until the mold was full. Finally, the sample was subjected to compression by machine again under two conditions: cold-pressed (CO) at room temperature and hot-pressed (HO) at 80°C with a pressure of 3.0–4.0 MPa for 10 min. These compressed samples (CO and HO) were incubated for 5 days to achieve homogenous colonization and then dried at 70°C for 24 to 72 h to stop colonization.

All products were weighed, and their dimensions were measured before and after drying. The density of mycelium-based biofoams derived from CC and SW sawdust fell within the range of 0.2 to 0.3 g/cm^3, while those derived from CW sawdust were in the range of 0.1 to 0.3 g/cm^3. A comprehensive overview of the mycelium-based biofoams preparation process for this study is shown in Fig. 2.

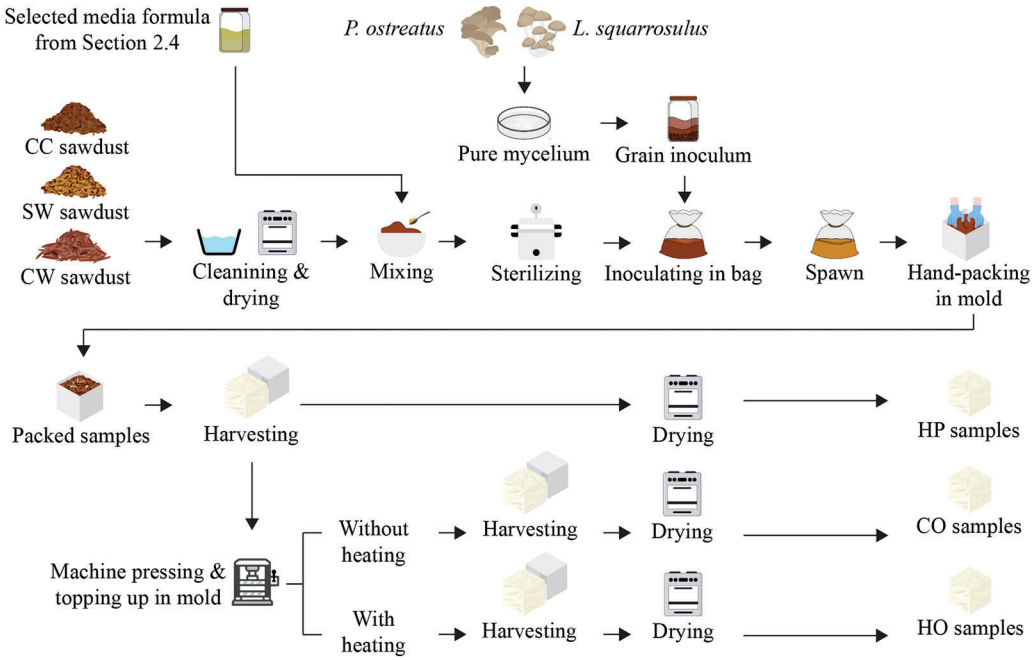

Figure 2: An overview of mycelium-based biofoams preparation process

2.6 Characterization of Mycelium-Based Biofoams

2.6.1 Appearance

Photographs of each sample were taken to record changes in the appearance of mycelium-based biofoams at different times, including during cultivation and at the final product stage.

2.6.2 Density and Shrinkage

The density of mycelium-based biofoams before and after dying was calculated by measuring the weight and volume of the samples. To measure the average shrinkage, the volumes before and after drying were calculated. Both parameters were determined using Eqs. (2) and (3), respectively.

$$\text{Density } \left(\text{g/cm}^3\right) = \frac{\text{Weight (g)}}{\text{Volume (cm}^3\text{)}} \tag{2}$$

$$\text{Average shrinkage (\%)} = \left(\frac{\text{V1} - \text{V2}}{\text{V1}}\right) \times 100 \tag{3}$$

where V1 is the original volume and V2 is the volume after drying.

2.6.3 Morphological Analysis

The morphology of mycelium fibers grown on different solid culture media, as well as the cross-sections of all mycelium-based biofoams, were analyzed using a scanning electron microscope (FEI Quanta 400 SEM) at an accelerating voltage of 20 kV. A thin layer of mycelium fibers (approximately 1 mm) was taken from the center of the sample surface and mounted on a platform using conductive adhesive tape, with the air-exposed side facing outwards. Cross-sectional samples of mycelium-based biofoams were also prepared. Both the mycelium fibers and cross-sectional biofoams were coated with a thin layer of gold-palladium to enhance the conductivity and imaging quality. The average diameter of the hyphae was calculated using the ImageJ software.

2.6.4 Fourier-Transform Infrared Spectroscopy (FT-IR)

The chemical composition of the sawdust types and mycelium-based biofoams was analyzed using a Fourier transform infrared spectrometer (Bruker, Alpha II) in the range of 4000–500 cm^{-1} with a resolution of 1 cm^{-1}.

2.6.5 Compressive Strength

Referring to ASTM C165-07, the compressive strength of the mycelium-based biofoams was determined using a universal testing machine (Tinius Olsen H10KS). The speed of loading head movement was set to 12.7 mm/min. The force applied to the sample was measured at 10% deformation.

2.6.6 Flexural Strength

Referring to ASTM C165-07, the compressive strength of the mycelium-based biofoams was determined using a universal testing machine (Tinius Olsen H10KS). The speed of loading head movement was set to 12.7 mm/min.

2.6.7 Water Absorption

The water absorption of mycelium-based biofoams was determined according to ASTM D570-98. Initially, the sample was weighed and completely immersed in water at room temperature for 24 h. Subsequently, the specimen was removed and wiped to eliminate excess water, and the final mass was recorded. Water absorption was calculated using Eq. (4).

$$\text{Water absorption } (\%) = \left(\frac{\text{Wf} - \text{Wi}}{\text{Wi}}\right) \times 100 \tag{4}$$

where Wi is the initial weight of the sample and Wf is the final weight of the sample.

2.6.8 Water Contact Angle (WCA)

The water contact angle was measured by dropping distilled water (5 mm in diameter) onto the surface of each sample using a syringe. Images of the droplets were taken and analyzed using ImageJ software.

2.6.9 Statistical Analysis

Data from each study, including mycelium growth rate and mycelium-based biofoam characteristics, were analyzed using one-way analysis of variance (ANOVA). Duncan's multiple range test was employed to identify significant differences ($p < 0.05$).

2.7 Cushion Factor

The quasi-static compression test of the mycelium-based biofoams, EPS foam (density of 0.01 g/cm^3), PE foam (density of 0.02 g/cm^3), and four stacks of double-wall BC flute corrugated board was performed according to ASTM D3574-05. The stress-strain curve was generated by applying loads of 65% deformation. The speed was 12.7 mm/min. The cushion factor was calculated using the stress-strain curve and Eqs. (5) and (6), respectively.

$$C = \left(\frac{G}{h/t}\right) = \frac{\sigma_m}{e_{load}} \tag{5}$$

$$e_{load} = \int_0^E \sigma dE \tag{6}$$

where C is the cushion factor, G is the ratio of acceleration a to gravity acceleration g, h (cm) is the drop height, t (cm) is the foam thickness, σ_{max} (MPa) is the maximum stress, and e_{load} (MPa) is the energy density.

3 Result and Discussion

3.1 Evaluation of Mycelium Growth Rate Grown on Different Formulations

3.1.1 Growth Rate of Mycelium Fibers

The growth period for mycelium fibers to fully cover a Petri dish (90 mm in diameter) ranged from the shortest time of 6 days to the longest period of 9 days, as shown in Table 1. The control treatment, which contained only sawdust and lacked additional nutrients, exhibited a significantly slower growth rate compared to the cultivated culture media. The types of sawdust and culture media formulas significantly affected the growth rate of both mushroom species. The growth rate of *P. ostreatus* was relatively consistent across the different sawdust types and culture media formulas, with slight variations, as shown in Fig. 3. However, the growth diameter of *L. squarrosulus* varied more significantly, especially with CW sawdust, which showed a higher growth rate in both formulas than in CC and SW sawdust (Fig. 3). Both species generally showed the highest growth rates in the CW sawdust. Furthermore, *L. squarrosulus* exhibited faster growth than *P. ostreatus* for all formulas, particularly CW sawdust (Fig. 4). This observation is consistent with the findings of Aiduang et al. [9], who reported higher growth rates of *Lentinus sp*. to *Pleurotus sp*. on sawdust substrates. Thus, both mushroom species displayed the highest growth rates in bran formula, particularly CW sawdust. This can be attributed to the lower lignin content of the CW sawdust (16% on a dry weight basis), which could be more easily facilitated and utilized by the mycelium fibers. This is consistent with previous studies that reported that a high lignin content may impede the breakdown of lignin, thus limiting its availability as a nutrient source [10,11], compared to the other two types of sawdust with lignin contents ranging from approximately 20% to 30% dry basis. Bran formula, containing sawdust and bran as primary carbon sources, provided a more sustained release of nutrients than dextrose formula, which relied on dextrose and yeast extract. Moreover, wood sawdust and bran contain complex carbohydrates that support long-term growth, whereas dextrose can degrade and be consumed more rapidly. According to Joshi et al. [12], wheat bran is rich in nutrients, and the incorporation of wheat bran as a component has proven advantageous, contributing essential nutrients that further support colonization. They found that wheat bran promoted the highest and fastest growth of *P. ostreatus*. Wongjiratthiti and Yottakot [13] demonstrated that carbohydrates, energy, minerals, and vitamins are key factors influencing fungal growth. In addition, *P. ostreatus* showed a slight variation in growth rate among the different sawdust types and culture media formulas, whereas *L. squarrosulus* showed a statistically significant difference in the growth rate of CW sawdust and bran formula.

Table 1: Mycelium growth rates of *P. ostreatus* and *L. squarrosulus* cultivated using various media formulas

Mushroom species	Media formulas	Sawdust type	Growth length (mm)	Growth period (days)	Growth rate (mm/day)
P. ostreatus	Control	CC	90	12	7.08 ± 0.00^{a}
		SW	90	11	7.73 ± 0.00^{b}
		CW	90	11	7.73 ± 0.00^{b}
	Bran	CC	90	9	9.57 ± 0.12^{c}
		SW	90	8	10.79 ± 0.13^{e}
		CW	90	8	10.83 ± 0.19^{e}
	Dextrose	CC	90	9	9.56 ± 0.06^{c}
		SW	90	9	9.51 ± 0.06^{c}
		CW	90	8	10.65 ± 0.02^{d}
L. squarrosulus	Control	CC	90	10	8.50 ± 0.00^{a}

(Continued)

Table 1 (continued)

Mushroom species	Media formulas	Sawdust type	Growth length (mm)	Growth period (days)	Growth rate (mm/day)
		SW	90	9	9.44 ± 0.00^{b}
		CW	90	8	10.63 ± 0.00^{c}
	Bran	CC	90	7	12.38 ± 0.22^{e}
		SW	90	7	12.29 ± 0.14^{e}
		CW	90	6	14.37 ± 0.03^{f}
	Dextrose	CC	90	9	9.46 ± 0.02^{b}
		SW	90	8	10.90 ± 0.34^{d}
		CW	90	6	14.37 ± 0.06^{f}

Note: Different lowercase letters indicate significant differences between treatments ($p < 0.05$). CC: commercial wood sawdust; SW: surface wood sawdust; CW: core wood sawdust.

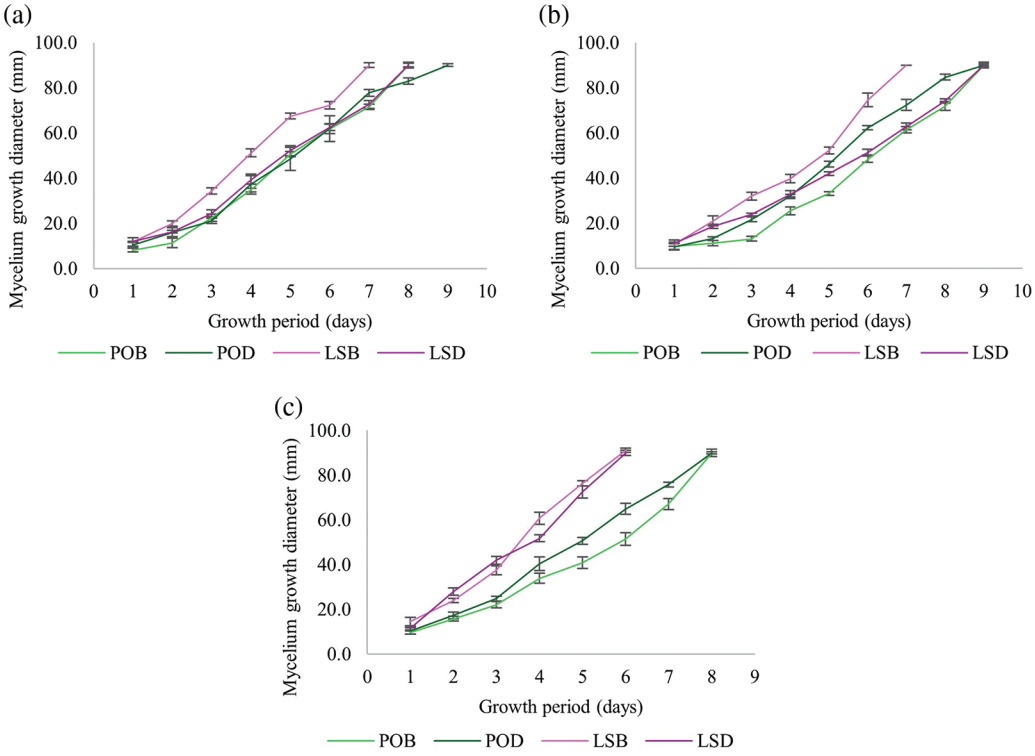

Figure 3: Mycelium growth diameter of *P. ostreatus* and *L. squarrosulus* cultivated on (a) CC (commercial wood sawdust); (b) SW (surface wood sawdust); (c) CW (core wood sawdust)

Note: POB: *P. ostreatus* in bran formula; POD: *P. ostreatus* in dextrose formula; LSB: *L. squarrosulus* in bran formula; LSD: *L. squarrosulus* in dextrose formula.

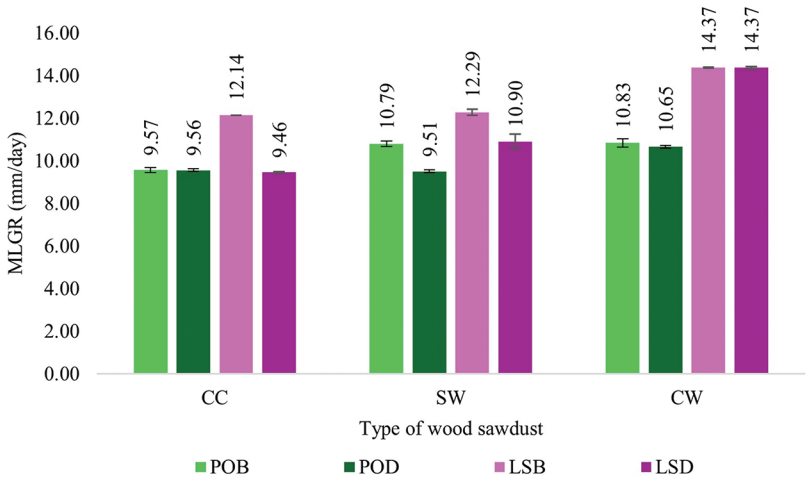

Figure 4: Mycelium linear growth rates of *P. ostreatus* and *L. squarrosulus*
Note: POB: *P. ostreatus* in bran formula; POD: *P. ostreatus* in dextrose formula; LSB: *L. squarrosulus* in bran formula; LSD: *L. squarrosulus* in dextrose formula.

3.1.2 Morphological Analysis of Mycelium Fibers

Hyphae are individual thread-like structures that make up the mycelium. Fig. 5 shows a detailed view of the cross-sectional structure of the fungal network and distribution of hyphal diameters. The largest and smallest diameters of the hyphae developed from each mushroom species are also displayed. The hyphae appeared densely packed and highly entangled, indicating strong growth of *P. ostreatus* cultivated on CC sawdust supplemented with bran formula. Hyphae diameters were relatively consistent, with a narrow distribution around the central peak, suggesting uniform growth with the thickest diameter of 1.62 µm (Fig. 5a). In contrast, a less dense network with some gaps and variations in hyphal thickness was observed in *P. ostreatus* cultivated on CW sawdust with dextrose formula because of the less uniform diameter distribution with the smallest diameter of 1.53 µm (Fig. 5b). The hyphae of *L. squarrosulus* cultivated on SW sawdust with bran formula were densely packed with a somewhat uniform distribution. Hyphae diameters were relatively consistent, but had a slightly broad distribution, with the thickest diameter of 1.77 µm (Fig. 5c). The broadest distribution and thinnest diameter of hyphae (1.60 µm) were found in *L. squarrosulus* cultivated on CW sawdust with dextrose formula. A thin mycelium network with significant gaps and irregularities in hyphal thickness was observed (Fig. 5d). The CC and SW sawdust appeared to support more uniform hyphal growth than the CW sawdust. This might be due to differences in the physical and chemical properties of sawdust types, which affect nutrient availability and hyphal attachment. Interestingly, biofoams cultivated on CW sawdust exhibited the fastest mycelium growth rate, and the diameter of the hyphae obtained was very thin. This finding can be associated with that of a study by Carlile et al. [14], who observed that a high degree of mycelium growth was correlated with high hyphal extension. This extension was influenced by the shape and size of the sawdust particles, with larger particles potentially leading to looser substrate uniformity. Consequently, the substrate may contain large gaps that facilitate the formation of individual filament networks and excess oxygen accumulation within the substrate. In contrast, dense substrates may limit mycelium growth [15]. Another possible reason for the slower growth observed in CC and SW sawdust is that more energy is directed toward producing the necessary enzymes for lignin degradation. This energy-intensive process limits the resources available for rapid hyphal extension, resulting in a slower overall growth rate. To efficiently penetrate and navigate the dense substrate, the mycelium adapts by developing thicker hyphae. These thicker hyphae provide the structural strength necessary for the mycelium to thrive in challenging environments, balancing the energy investment between enzyme production and structural support. The

bran formula generally supported denser and more uniform hyphal growth than the dextrose formula. This could be because of the higher nutrient content and better suitability of the bran for fungal growth.

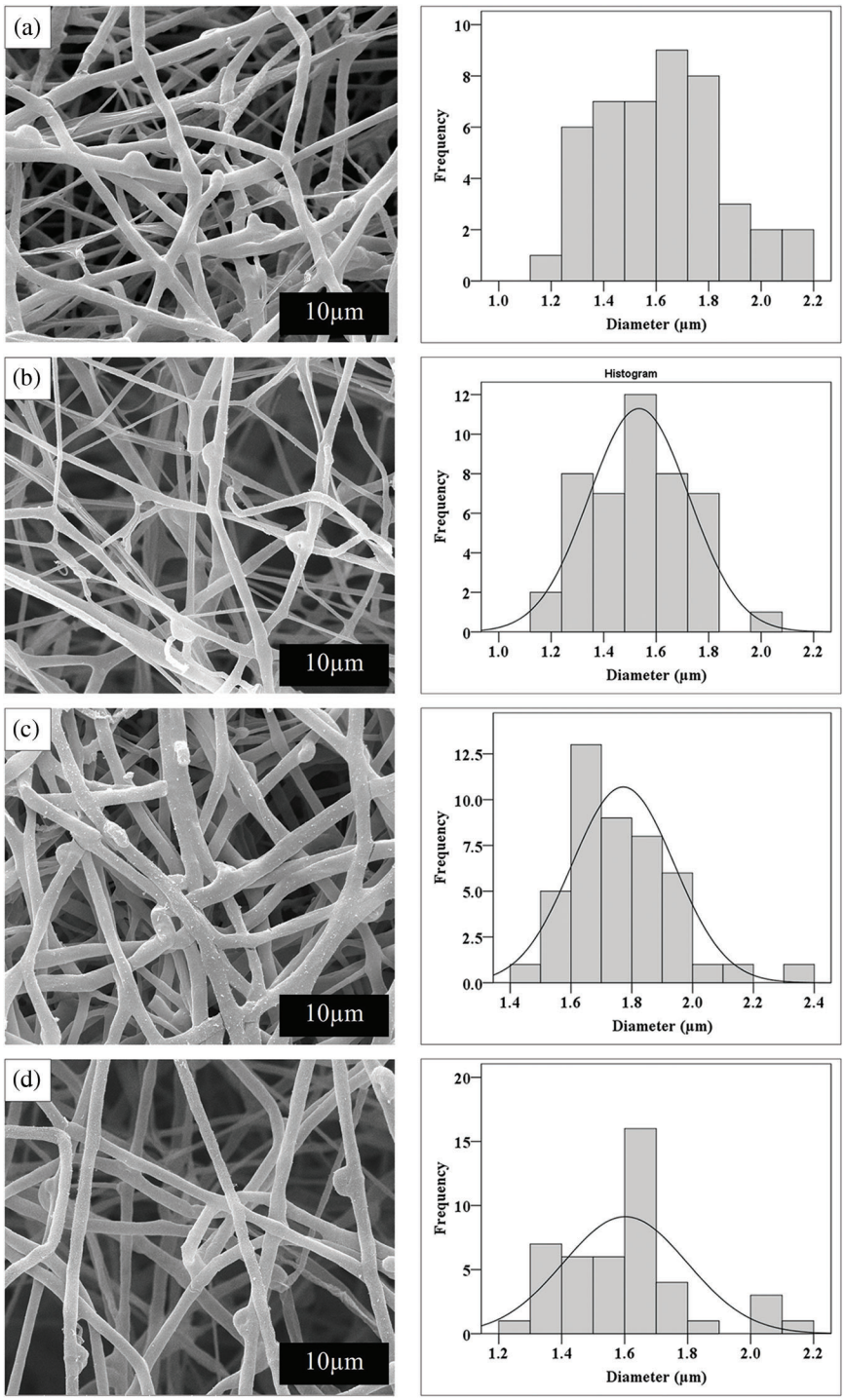

Figure 5: SEM images and frequency distribution of hyphae diameters of (a) *P. ostreatus* cultivated on CC (commercial wood sawdust) using bran formula (b) *P. ostreatus* cultivated on CW (core wood sawdust) using dextrose formula (c) *L. squarrosulus* cultivated on SW (surface wood sawdust) using bran formula and (d) *L. squarrosulus* cultivated on CW (core wood sawdust) using dextrose formula (scale bar 10 µm)

3.2 Characterization of Mycelium-Based Biofoams

3.2.1 Appearance

The appearance of the mycelium-based biofoams during cultivation is shown in Fig. 6. In general, biofoams derived from *L. squarrosulus* appeared to change to white mycelium, covering faster than those from *P. ostreatus*. Significant changes were observed within 3 days, and the biofoams fully covered the white mycelium within 10 days. The first stage of mycelium expansion involves absorption of small molecules by hyphae as they grow. These molecules are digested by the prevailing enzymes secreted from the hyphal tips to support growth and metabolism. Hyphae then extend their filaments and fuse them to form a network [16]. As hyphae continued to grow and branch neighboring hyphae together, the mycelium expanded throughout the substrate and gradually covered it until day 10. The biofoams exhibited a thicker layer of white fibers, particularly those produced from *L. squarrosulus*. In contrast, biofoams derived from *P. ostreatus* showed less hyphal coverage. For both mushroom species, biofoams made with CC and SW sawdust exhibited denser and more uniform mycelium growth than those made with CW sawdust. This was evident in the images in Fig. 6 showing the progression of mycelium growth from day 3 to day 10 (A1-D1 and A2-D2), where the CC and SW sawdust biofoams displayed a more homogeneous and compact appearance. In contrast, biofoams made with CW sawdust showed less dense and more irregular mycelium growth with visible sawdust particles and a more heterogeneous structure (A3-D3). This was particularly noticeable in the images of the 10-day biofoams before drying (D1-D3) and the cold-pressed and hot-pressed samples on day 15 before drying (E1-E3 and F1-F3). The differences in mycelium growth and biofoam appearance can be attributed to the properties of sawdust types. CC and SW sawdust are likely to have a more favorable composition and particle size distribution for mycelium growth, allowing for better colonization and binding of the substrate. Additionally, they efficiently colonize these substrates because of their ability to produce enzymes for lignin degradation and develop thicker hyphae, which promotes successful colonization. CW sawdust may have less suitable properties. The larger particle size of CW sawdust requires mycelium to cover larger individual particles, thereby extending the time needed for full colonization of the substrate. While the gaps between these larger particles facilitate easier penetration and spreading of the hyphae, the overall process of bridging these gaps and covering the expanded surface area leads to slower and more uneven mycelium growth.

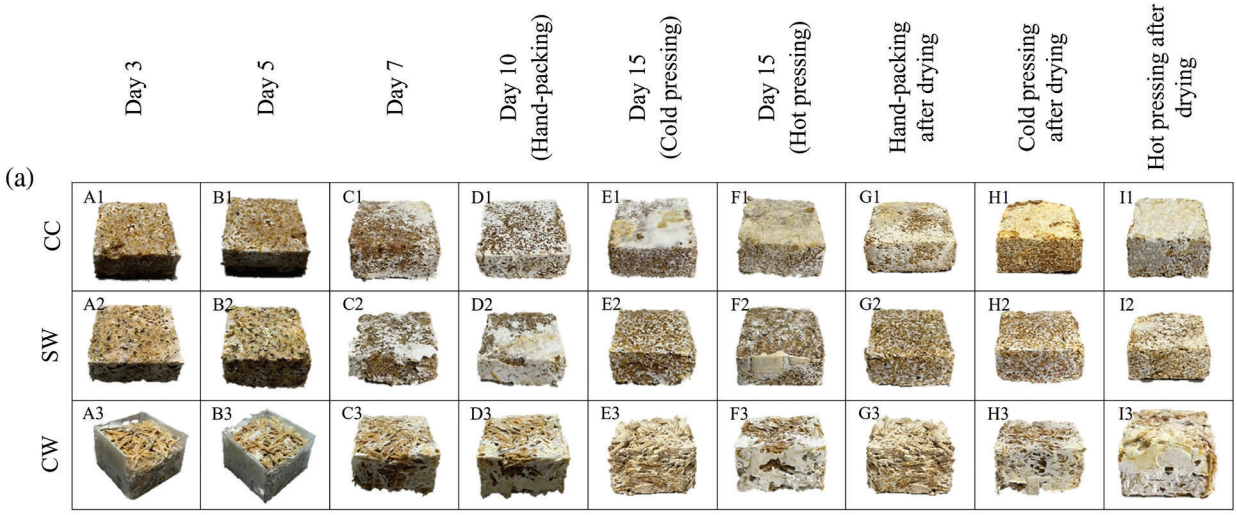

Figure 6: (Continued)

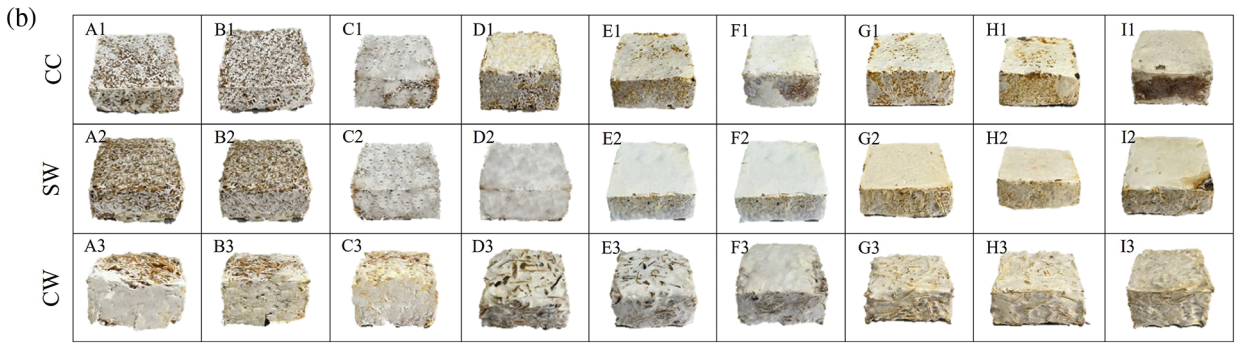

Figure 6: Changes in mycelium-based biofoams produced by (a) *P. ostreatus* and (b) *L. squarrosulus* cultivated on various wood sawdust types during incubation

Note: A1-A3: for 3 days incubation, B1-B3: for 5 days incubation, C1-C3: for 7 days incubation, D1-D3: samples from hand-packing (HP) and 10 days incubation, E1-E3: samples from cold pressing (CO) and 15 days incubation, F1-F3: samples from hot pressing (HO) and 15 days incubation, G1-G3: samples from hand-packing (HP) and after drying, H1-H3: samples from cold pressing (CO) and after drying, and I1-I3: samples from hot pressing (HO) and after drying, CC: commercial wood sawdust, SW: surface wood sawdust, and CW: core wood sawdust.

Biofoams pressed by HP (G1-G3), CO (H1-H3), and HO (I1-I3) in Fig. 6 after drying exhibited variations in appearance which were significantly influenced by sawdust type and pressing method. CC and SW sawdust offered a more uniform and compact structure, whereas CW sawdust appeared more porous and less cohesive. In terms of pressing, CO improved the uniformity but was not as effective as HO, which produced the most compact and homogeneous biofoam appearance, especially for *L. squarrosulus*. In contrast, the surface of the biofoams derived from *P. ostreatus* showed an enhanced rigid appearance but remained sparsely covered. This difference could be attributed to *L. squarrosulus* having a faster growth rate than *P. ostreatus*, which allowed sufficient time for extensive hyphal expansion before pressing. Therefore, CC-HO and SW-HO promote a more homogeneous and compact biofoam structure. In addition, all the demolded biofoams from *L. squarrosulus* typically displayed a uniform white to off-white coloration with a smooth surface texture, indicative of consistent mycelium growth. Conversely, biofoams from *P. ostreatus* exhibited a light beige color and rough skin, which is consistent with observations reported in a study by Appels et al. [17]. After drying, the surfaces of all mycelium-based biofoams were yellowish because of the Maillard reaction in the presence of sugars and proteins in the mycelium cell wall composition. This discoloration could also be caused by the caramelization of polysaccharides in the wood sawdust substrates [18].

3.2.2 Morphological Analysis

Cross-sectional views of mycelium-based biofoams examined using SEM are shown in Fig. 7. These images provide insights into the effects of wood sawdust types and pressing methods on the microstructure of mycelium-based biofoams. Biofoams from HP (A1-A4 in Fig. 7) generally have larger and more irregular air voids, indicating less compression and more space within the structure. On the other hand, CO and HO (B1-B4 and C1-C4 in Fig. 7) offered biofoams with a more compact structure, smaller air voids, and a more uniform distribution of mycelium. In addition, HO provided the most compact and dense structure with minimal air voids, resulting in significant compression of mycelium and sawdust. Thus, compression reduced the porosity of the biofoams, leading to a more homogeneous and compact structure. In addition, compression facilitated the alignment of the fibers and sawdust particles in a more organized structure, thereby enhancing the structural integrity of the biofoams. Consequently, the biofoams were more resistant to deformation and shrinkage while also increasing their

density. Biofoams from CC sawdust exhibited the most significant decomposition and smallest voids, indicating the highest level of fungal activity and integration, especially in hot pressing (D1 in Fig. 7), whereas CW sawdust offered larger voids and more undecayed substrate across all pressing methods (D4 in Fig. 7), respectively, indicating less effective decomposition by mycelium.

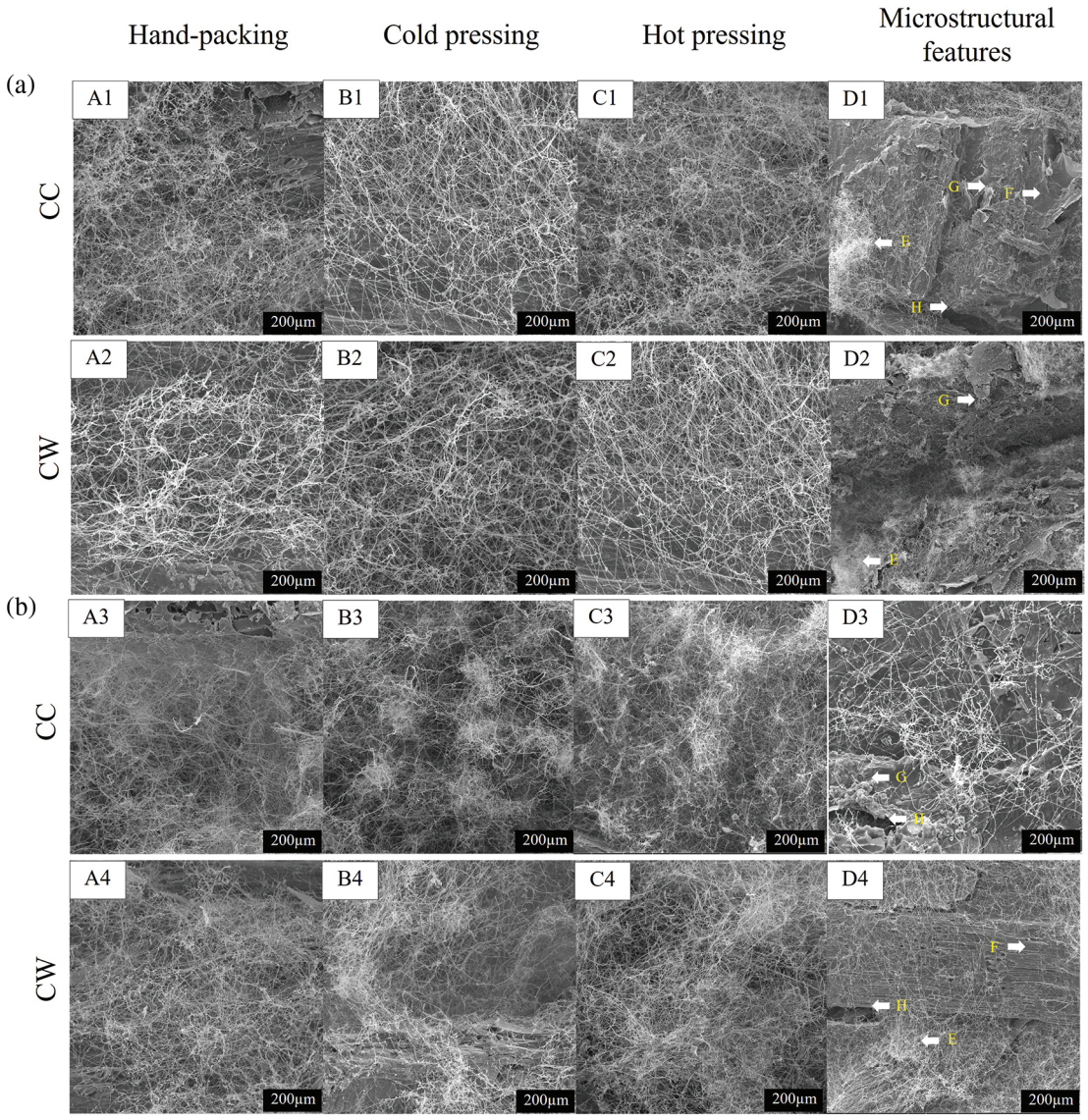

Figure 7: SEM images of mycelium-based biofoams produced by (a) *P. ostreatus* and (b) *L. squarrosulus* cultivated on various sawdust types (scale bar 200 μm)

Note: A1-A4: samples from hand-packing (HP), B1-B4: samples from cold pressing (CO) samples, C1-C4: samples from hot pressing (HO), D1-D4: microstructural features of samples from hot pressing, E: fungal mycelium, F: undecayed substrate, G: degraded substrate, H: air-void.

The hot-pressed samples displayed diminished visibility of individual fibers due to the bonding between the hyphae and substrates after hot pressing, as shown in Fig. 7 D1-D4 [17]. Furthermore, the presence of fewer mycelium fibers in the center of the biofoams was related to the limited flow of oxygen into the

substrates, which slowed mycelium growth. Another possible reason is that the hyphae penetrated each sawdust particle and were degraded by the enzymes [19]. From the appearance of the samples in Fig. 7, it was observed that the exterior surface of the mycelium-based biofoams derived from *P. ostreatus* did not show extensive fiber coverage. However, the internal structures revealed the presence of interwoven networks. This observation is consistent with the study by Alemu et al. [20], who found that the pure sawdust morphology exhibited numerous voids. In contrast, the biofoams exhibited fewer voids because of the interconnection of the fibers within the structure. Therefore, hot pressing (HO), particularly with cultivated wood sawdust, results in the most compact and dense biofoam because of efficient fungal decomposition and integration of the substrate.

3.2.3 Fourier-Transform Infrared Spectroscopy

The FTIR spectra of mycelium-based biofoams produced from *P. ostreatus* and *L. squarrosulus* cultivated on different types of sawdust and subjected to various pressing methods are shown in Fig. 8. Sawdust is composed of cellulose, hemicellulose, lignin, organic compounds (tannins and phenolic compounds), inorganic minerals, moisture, proteins, and starches [21]. As shown in Fig. 8, the characteristic peaks of the substrates studied (CC, SW, and CW) are as follows. A broad peak around 3300 cm^{-1}, indicative of the O-H stretching of hydrogen bonds, was prominently observed. These were attributed to cellulose, hemicellulose, moisture, and lignin in the sawdust. The peak at 3000–2800 cm^{-1} was assigned to C-H stretching in waxes and oils in sawdust. The peak at 1750 cm^{-1} was attributed to C=O stretching, which was associated with carbonyl groups, indicating proteins and lignin. The peak around 1510–1600 cm^{-1} was assigned to C=C stretching, related to aromatic rings, typically from lignin and phenolic compounds. The peaks between 1000 and 1300 cm^{-1} were assigned to C-O stretching, indicating the presence of C-O bonds in the polysaccharides.

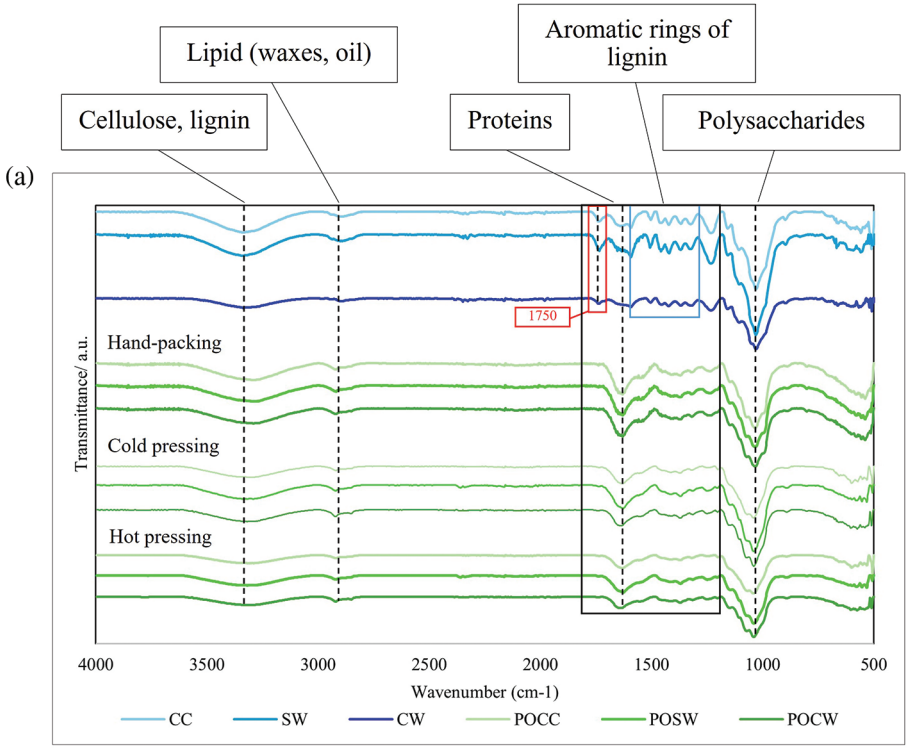

Figure 8: (Continued)

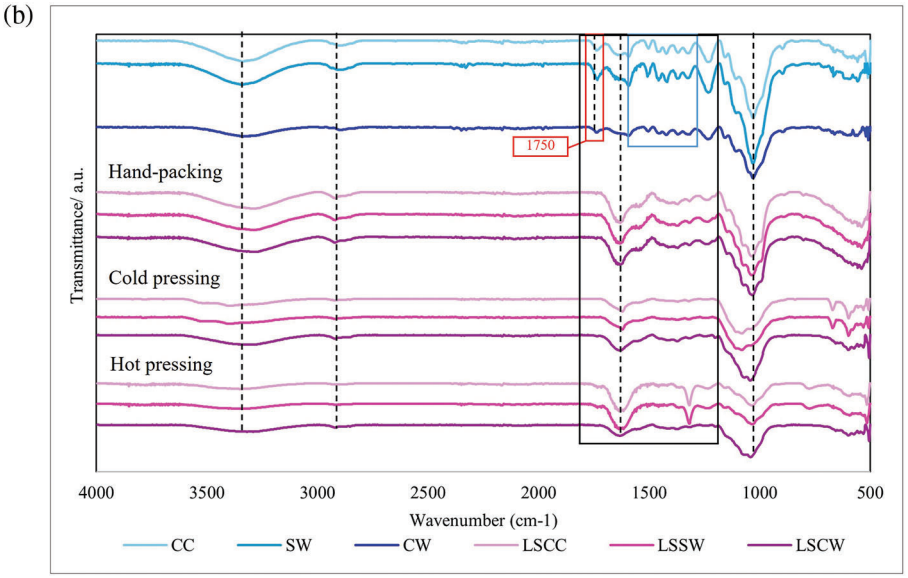

Figure 8: FTIR spectra of mycelium-based biofoams produced by (a) *P. ostreatus* (PO) and (b) and *L. squarrosulus* (LS) cultivated on various sawdust types

Note: CC: commercial wood sawdust, SW: surface wood sawdust, and CW: core wood sawdust, POCC: *P. ostreatus* cultivated on commercial wood sawdust, POSW: *P. ostreatus* cultivated on surface sawdust, POCW: *P. ostreatus* cultivated on core wood sawdust, LSCC: *L. squarrosulus* cultivated on commercial wood sawdust, LSSW: *L. squarrosulus* cultivated on surface wood sawdust, LSCW: *L. squarrosulus* cultivated on core wood sawdust.

CC sawdust showed prominent and well-defined absorption bands compared to SW and CW sawdust. The CC sawdust spectra exhibited distinct and sharp bands at around 3300 cm^{-1}, 3000–2800, 1750, and 1000 cm^{-1}, indicating a more uniform, ordered, and crystalline structure in the sawdust. In contrast, the SW and CW sawdust spectra showed broader and less intense bands, suggesting a more amorphous and heterogeneous composition. In addition, the CW spectra generally showed significant broadening and less intense peaks for C=O and C-O stretching, indicating lower lignin, protein, and polysaccharide contents. A comparison of the FTIR spectra of sawdust and biofoams revealed significant chemical transformations owing to mycelium colonization and pressing methods. The intensities at 3300 cm^{-1} (hydroxyl groups of cellulose, moisture, and lignin), 1750 cm^{-1} (carbonyl groups of protein and lignin), and 1550 cm^{-1} (aromatic rings in lignin) in biofoams were weaker than those in sawdust. This is because mycelium growth primarily relies on the consumption of lignin, cellulose, and hemicellulose present in the substrate [4,22]. The degradation of these components indicated the enzymatic breakdown of the polysaccharide matrix and lignin structure caused by mycelium enzymes. These results were consistent with the findings of Haneef et al. [23], who reported similar transformations in lignocellulosic materials subjected to biological decay. Notably, the pure sawdust spectra showed sharper and more defined O-H stretching peaks compared to the biofoam samples, suggesting that the enzymatic activity of mycelium hyphae significantly altered the hydrogen bonding network in the sawdust. Proteins were identified by the amide I band around 1700–1600 cm^{-1}, amide II and III bands between 1575–1300 cm^{-1}, and NH_2 stretching vibration at 1320 cm^{-1}. These peaks highlighted the presence of mycelium proteins within the biofoams, consistent with the findings of Haneef et al. [23]. The amide bands indicated protein secondary structures, which were essential for the mechanical stability and functional properties of mycelium-based biofoams. In contrast, the sawdust showed very low-intensity peaks in these regions, emphasizing the introduction

of proteinaceous material by the mycelium and the transformation of the sawdust matrix into a protein-rich biofoam. Furthermore, nucleic acids were detected around 1255–1245 cm^{-1}, although their presence was less pronounced than that of other biomolecules. This region corresponded to the phosphate vibrations within nucleic acids, as reported by Pena et al. [24] and Galichet et al. [25]. The subtle presence of these peaks suggested minimal but notable genetic material within mycelium biomass. These peaks were largely absent in the pure sawdust spectra, indicating that the introduction of nucleic acids was a direct result of mycelium colonization and growth, as reported by Peng et al. [4] and Schwanninger et al. [26]. The reduction in intensity at 1550 cm^{-1} indicated the breakdown of lignin, which is consistent with report by Peng et al. [4]. The enzymatic activity of the mycelium facilitated the degradation of lignin, leading to the formation of more accessible and reactive functional groups.

The FTIR spectra for biofoams from both mushroom species indicated that the overall chemical composition was primarily influenced by the sawdust type and pressing method. Both species exhibited similar trends. A higher content of structural components (lignin and cellulose) was observed in biofoams prepared from CC and SW sawdust, whereas a lower content was observed in biofoams made from CW sawdust. The O-H, C-H, C=O, and C-O stretching peaks, indicating a high hydroxyl content, aliphatic compounds, carbonyl group, and polysaccharides, were sharply displayed in biofoams pressed by HP, while biofoams prepared by mechanical pressing exhibited gradually less intensity, particularly in biofoams pressed by HO. The reduction in the O-H, C-H, and C-O peaks indicated some level of thermal degradation of the organic components. This degradation could lead to changes in the mechanical properties, making biofoams more rigid and less flexible. Furthermore, significant dehydration and reduction in the hydroxyl content can improve the moisture barrier of biofoams. Moreover, the core structures of the biofoams, as indicated by the C=O and C-O peaks, remained relatively intact. This suggests that HO enhances the compactness and potentially the mechanical strength of biofoams. Therefore, HO significantly altered the chemical structure of mycelium-based biofoams as a result in enhanced chemical stability, structural integrity, and performance characteristics.

3.2.4 Density and Shrinkage

Table 2 presents the density before and after drying of mycelium-based biofoams prepared using different types of sawdust and pressing methods. The density before and after drying varied depending on the type of sawdust and pressing method used. The highest density of mycelium-based biofoams for *P. ostreatus* and *L. squarrosulus* before drying was observed in hot-pressed samples using commercial wood sawdust (CC-HO) and surface wood sawdust (SW-HO), at 0.77 g/cm^3 whereas, the lowest density before drying was found in hand-packing with core wood sawdust (CW-HP) for both mushroom species, at 0.54 and 0.53 g/cm^3, respectively. Similar trends were observed in post-drying, with the highest density recorded for SW-HO at 0.31 and CC-HO at 0.30 g/cm^3, and the lowest for CW-HP at 0.20 and 0.17g/cm^3, respectively. The densities obtained from both mushroom species were similar to those reported in previous studies on hand-packed samples [4,9,12]. The densities of the cold pressed and hot pressed samples were comparable to those reported by Appels et al. [17] and Aiduang et al. [9]. Several studies support the results of this study, indicating that pressing methods (cold pressing and hot pressing) significantly increase the density of mycelium-based biofoams [8,9,17,27]. The density of the pre-dried samples was primarily influenced by the moisture content in the substrates, resulting in a slight variation in density across the samples cultivated on different types of wood sawdust. However, the removal of water after drying led to a reduction in the biofoams weight. The variations in the densities of the post-dried mycelium-based biofoams can be attributed to the particle size and shape of wood sawdust. Both CC and SW sawdust had smaller particles ranging from 1 to 2 mm in length. This smaller particle size likely contributed to a more consistent and compact arrangement of the particles, resulting in a denser

structure in the post-drying samples. The uniformity of the smaller particles can reduce the occurrence of voids, allowing for more efficient packing and reducing the spaces where moisture can be retained. In contrast, CW sawdust had larger particles, which might have led to less uniformity, creating larger voids within the structure. These voids facilitate the removal of moisture during the drying process, resulting in a lower density. Shrinkage is another critical factor that is affected by the type of sawdust and pressing method. The highest shrinkage was observed in CC-HP for *P. ostreatus* (14.84%) and CC-HP for *L. squarrosulus* (13.62%), whereas the lowest shrinkage was found in CW-HO for both mushroom species (9.90% and 7.17%), as shown in Table 2. Thus, the type of sawdust and pressing method significantly affected the shape stability of the mycelium-based biofoams. These results agreed with several studies, which reported that the normal average shrinkage of mycelium-based materials ranged from 5.10%–20.00% [8,28]. Nava et al. [28] reported that low average shrinkage is correlated with material stability. In this study, hot pressing resulted in the lowest average shrinkage, followed by cold pressing, and hand packing. Hot pressing generally results in higher density and lower shrinkage than other pressing methods because of the greatest material stability. Furthermore, CC sawdust tended to have a higher density and higher shrinkage. CW sawdust, especially when hot-pressed, led to significantly lower shrinkage and a moderately low density. Therefore, the CW-HP produced biofoams with characteristics of low density and low shrinkage.

Table 2: Density and average shrinkage of mycelium-based biofoams

Mushroom species	Sawdust type	Pressing method	Density before drying (g/cm^3)	Density after drying (g/cm^3)	Average shrinkage (%)
P. ostreatus	CC	HP	0.67 ± 0.01^{cd}	0.23 ± 0.01^{b}	14.84 ± 0.85^{e}
		CO	0.75 ± 0.01^{e}	0.26 ± 0.00^{c}	11.71 ± 1.50^{bc}
		HO	0.77 ± 0.02^{f}	0.30 ± 0.01^{d}	10.61 ± 1.50^{ab}
	SW	HP	0.68 ± 0.01^{d}	0.23 ± 0.01^{b}	13.86 ± 2.31^{de}
		CO	0.75 ± 0.01^{e}	0.27 ± 0.01^{c}	12.48 ± 1.72^{cd}
		HO	0.77 ± 0.03^{f}	0.31 ± 0.01^{d}	11.51 ± 0.01^{bc}
	CW	HP	0.54 ± 0.01^{a}	0.20 ± 0.02^{a}	11.12 ± 1.71^{abc}
		CO	0.66 ± 0.03^{b}	0.22 ± 0.01^{b}	11.86 ± 1.55^{bc}
		HO	0.67 ± 0.01^{bc}	0.27 ± 0.01^{c}	9.90 ± 0.80^{a}
L. squarrosulus	CC	HP	0.67 ± 0.02^{d}	0.22 ± 0.01^{b}	13.62 ± 2.50^{c}
		CO	0.74 ± 0.01^{e}	0.27 ± 0.01^{e}	11.46 ± 1.15^{b}
		HO	0.77 ± 0.02^{f}	0.30 ± 0.01^{f}	7.54 ± 1.54^{a}
	SW	HP	0.67 ± 0.01^{cd}	0.22 ± 0.01^{b}	13.51 ± 0.79^{c}
		CO	0.74 ± 0.01^{e}	0.27 ± 0.01^{de}	12.06 ± 1.74^{b}
		HO	0.77 ± 0.01^{f}	0.29 ± 0.01^{f}	7.27 ± 1.27^{a}
	CW	HP	0.53 ± 0.01^{a}	0.17 ± 0.01^{a}	10.79 ± 2.07^{b}
		CO	0.64 ± 0.01^{b}	0.24 ± 0.01^{c}	11.41 ± 1.30^{b}
		HO	0.66 ± 0.03^{c}	0.26 ± 0.01^{d}	7.17 ± 1.00^{a}

Note: Different lowercase letters indicate significant differences between treatments ($p < 0.05$). CC: commercial wood sawdust; SW: surface wood sawdust; CW: core wood sawdust, HP: hand-packing, CO: cold pressing, HO: hot pressing.

3.2.5 Compression and Flexural Strength

Analysis of the data in Table 3 shows that the factors studied significantly influenced the mechanical properties of the mycelium-based biofoams. The compression strength indicates the material's ability to withstand compressive forces, whereas flexural strength reflects the material's ability to resist deformation under a bending load. In terms of pressing methods, HO generally resulted in the highest compression and flexural strengths for both mushroom species and all sawdust types, followed by CO and HP. This is because HO offered greater compaction and improved structural integrity, whereas CO also enhanced the strength properties, but not as significantly as HO. In addition, HP exhibited the lowest strength, indicating less effective compaction and structural integrity. Regarding sawdust types, CC and SW sawdust generally provided higher compression and flexural strengths than CW sawdust for both mushroom species and all pressing methods. Statistical analysis confirmed that these factors had a significant impact on the mechanical performance of biofoams. The thinner diameter of hyphae grown on CW sawdust may hinder its effectiveness in promoting binding and achieving structural cohesion in biofoams, as they may not completely fill the spaces between particles of CW sawdust. This suggests that CW sawdust is less effective for binding and structural cohesion in biofoams.

Table 3: Compression and flexural strength of mycelium-based biofoams

Mushroom species	Sawdust type	Pressing method	Compression strength (MPa)	Flexural strength (MPa)
P. ostreatus	CC	HP	0.28 ± 0.02^{c}	0.15 ± 0.01^{b}
		CO	0.47 ± 0.03^{d}	0.19 ± 0.01^{d}
		HO	0.52 ± 0.02^{e}	0.22 ± 0.01^{e}
	SW	HP	0.28 ± 0.02^{bc}	0.15 ± 0.01^{b}
		CO	0.48 ± 0.03^{d}	0.19 ± 0.01^{d}
		HO	0.53 ± 0.02^{e}	0.22 ± 0.01^{e}
	CW	HP	0.21 ± 0.02^{a}	0.13 ± 0.01^{a}
		CO	0.26 ± 0.01^{b}	0.17 ± 0.01^{c}
		HO	0.47 ± 0.02^{d}	0.18 ± 0.01^{d}
L. squarrosulus	CC	HP	0.28 ± 0.02^{c}	0.16 ± 0.01^{b}
		CO	0.47 ± 0.02^{e}	0.20 ± 0.01^{d}
		HO	0.50 ± 0.02^{f}	0.23 ± 0.02^{e}
	SW	HP	0.27 ± 0.03^{bc}	0.16 ± 0.01^{b}
		CO	0.45 ± 0.03^{e}	0.20 ± 0.01^{d}
		HO	0.50 ± 0.03^{f}	0.22 ± 0.01^{e}
	CW	HP	0.19 ± 0.01^{a}	0.14 ± 0.01^{a}
		CO	0.26 ± 0.01^{b}	0.18 ± 0.01^{c}
		HO	0.44 ± 0.02^{d}	0.19 ± 0.01^{c}

Note: Different lowercase letters indicate significant differences between treatments ($p < 0.05$). CC: commercial wood sawdust; SW: surface wood sawdust; CW: core wood sawdust, HP: hand-packing, CO: cold pressing, HO: hot pressing.

The results demonstrated trends similar to those observed for density, suggesting a correlation between the density and compressive strength, as mentioned in the study by Ghasvinian et al. [29]. This correlation is likely due to low density and high porosity materials being more prone to deformation and crushing [4]. The

similar compression strengths of CC and SW sawdust suggest that the particle size of these sawdust types contributed to a more uniform structure, whereas a slightly lower value for CW sawdust indicated that a larger particle size might lead to less effective bonding within the biofoam structure. The use of mechanical pressing could promote strength, and the application of heat further improved mechanical stability. Apples et al. [17] found that heat pressing improves the homogeneity, strength, and stiffness of mycelium-based biofoams. Several studies have shown that heat increases the bonding between fungal hyphae and substrates. This was due to intermolecular hydrogen bonds formed by free radicals generated by lignin-degrading enzymes, which react with polysaccharides in the fungal cell wall, leading to the formation of cross-linked structures [30].

According to previous results, although the CW-HO biofoam had a lower density and percentage of shrinkage and larger air voids, which facilitated the bonding of individual mycelium fibers compared to other HO treatments, its mechanical properties were still inferior. This suggests that the type of sawdust plays a crucial role in determining the strength of biofoams, even when the air void content and density are favorable. Differences in the chemical composition and structure of CW sawdust may affect its bonding and compatibility with the mycelium. In addition, the potential disruption of the cellular structure because the presence of CW sawdust particles may result in a less homogeneous and weaker biofoam.

Mycelium-based biofoams, particularly those using CC and SW sawdust with CO and HO pressing methods, demonstrated compressive strengths comparable to those of biocomposite foams based on methyl cellulose, cellulose fibers, and lignin studied by Miranda-Valdez et al. [31], which had compressive strengths of 0.37–2.18 MPa. Mycelium biofoams also showed superior compressive strength compared to rigid foams reinforced with agricultural waste, such as rice husks and banana rachises examined by Lazo et al. [32], which only achieved 0.12–0.23 MPa. However, the flexural strengths of the mycelium biofoams were generally lower than those of other biocomposite materials. For instance, biodegradable rigid foams from pineapple field waste studied by Namphonsane et al. [33] achieved 1.5–4.5 MPa flexural strength, which exceeded those observed for the mycelium biofoams. The difference was even more pronounced when compared to wood-based materials such as particleboards. Pędzik et al. [34] reported particleboards incorporating walnut wood residues reached flexural strengths of approximately 19 MPa, substantially higher than the mycelium biofoams. Mycelium-based biofoams have demonstrated potential in terms of compressive strength; however, their flexural strength can be improved to enhance their competitiveness with a broader range of biocomposite materials. The elasticity of the mycelium structure likely contributes to its lower stiffness, but potentially greater flexibility compared to more rigid wood-based materials.

3.2.6 Water Absorption

The water absorption properties indicating porosity and hydrophilicity of mycelium-based biofoams prepared using different types of sawdust and pressing methods are shown in Fig. 9a. Biofoams pressed by HP generally exhibited the highest water absorption for both mushroom species and all sawdust types. The high water absorption can be attributed to the higher porosity and less compact structure of the HP samples, which allowed for greater water uptake. In contrast, HO offered significantly lower water absorption by biofoams made of CC and SW sawdust in both mushroom species, ranging from 108.29% to 124.34%. The CW sawdust tended to show significantly higher water absorption in all biofoams, possibly because of its higher porosity. The substantial reduction in water absorption by CO and HO suggests that the interfacial bonding between the mycelium fibers and the substrate improved with increasing [19]. Chemical analysis further supported this finding, showing a stronger intensity peak of hydroxyl groups for the HP samples, while the CO and HO samples displayed the weakest peak intensity. This indicates that the chemical composition and bonding within the material were influenced by the pressing method. The study also compared biofoams derived from the two species, which

showed similar trends in water absorption. However, there were subtle differences in the values, with biofoams made from *L. squarrosulus* absorbing less water than those made from *P. ostreatus*. This could be related to the appearance of the samples, as *L. squarrosulus* biofoams exhibited thicker fungal skin, which might have reduced water uptake. This observation was consistent with the study by Appels et al. [17], who found that bio-composites produced from *Tremetes multicolor* had the lowest water absorption due to high surface coverage. Furthermore, visual observation after immersing all the tested samples in water for 24 h did not show any fall off the substrate particles. This suggests that there were some pores and spaces inside the biofoams, allowing them to expand and hold water, as mentioned by Joshi et al. [12] and Peng et al. [4]. This ability to maintain structural integrity while absorbing water highlights the potential of mycelium-based biofoams for various applications that require moisture retention and resilience.

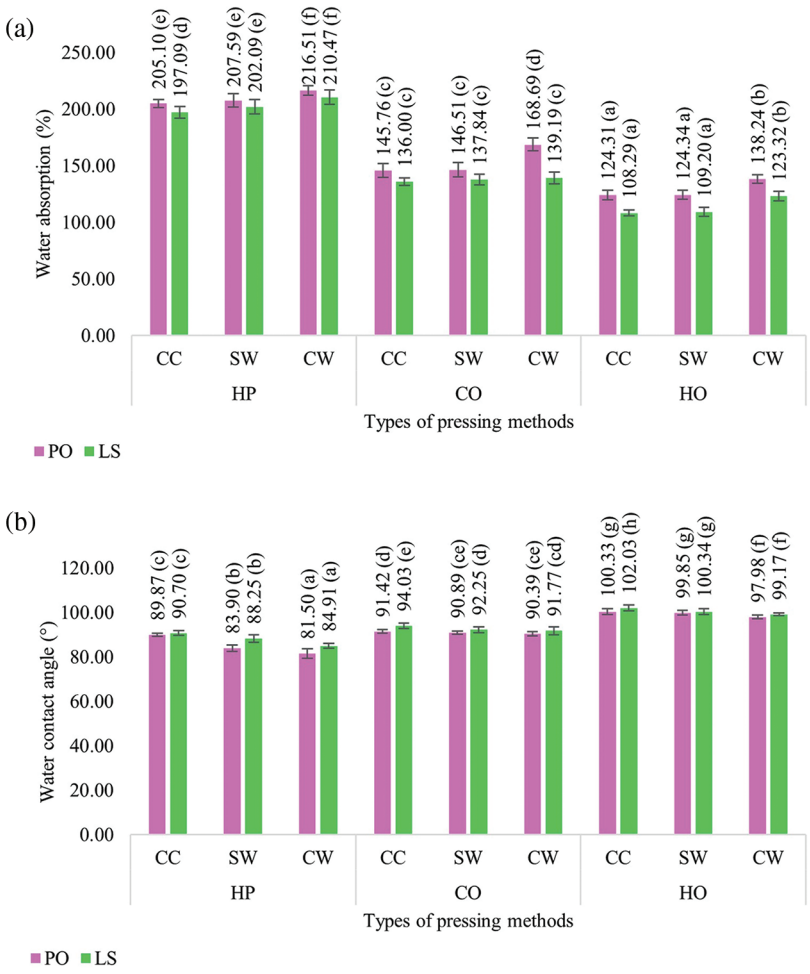

Figure 9: (a) Water absorption and (b) Water contact angle of mycelium-based biofoams produced by *P. ostreatus* (PO) and *L. squarrosulus* (LS) cultivated on various sawdust types and pressing methods

Note: Different lowercase letters indicate significant differences between treatments ($p < 0.05$). CC: commercial wood sawdust; SW: surface wood sawdust; CW: core wood sawdust, HP: hand-packing, CO: cold pressing, HO: hot pressing.

3.2.7 Water Contact Angle (WCA)

The hydrophobicity of the mycelium-based biofoam surface was determined using WCA, as shown in Fig. 9b. It was found that the overall WCA values were high, in the range of 81.50–102.03°, suggesting that the mycelium can improve the water resistance properties on the surface of the substrates. However, the biofoams pressed by HP were still classified as hydrophilic, owing to a WCA lower than 90°. The results were aligned with those of the bio-composites produced from *P. ostreatus* in a study by Peng et al. [4]. Interestingly, biofoams pressed by CO and HO in all sawdust types had WCA in the range 90°–102° which is the hydrophobic class. In addition, HO resulted in the highest water contact angle, indicating that it had the most hydrophobic surfaces. CO increased hydrophobicity compared to HP but was less than that of HO. Furthermore, CC-HO generally provided the highest contact angles, indicating that it had the most hydrophobic surfaces. CW-HO consistently exhibited the lowest contact angles, indicating a more hydrophilic surface. The pressing method and high temperature provided smoother surfaces and a better arrangement of the sawdust substrates. During hyphal growth, these fibers may form a more uniform and tightly bonded surface. This smoother, well-arranged surface contributed to increase hydrophobicity. Previous study has indicated that the external layer of pure mycelium is hydrophobic [35], which is attributed to a specific protein called hydrophobin. This protein self-assembles into a coating that covers the surface of aerial mycelium [36]. The characteristics of mycelium from mushroom species also indicate the effect on hydrophobicity. It was found that biofoams made from *L. squarrosulus* consistently displayed a higher WCA than those from *P. ostreatus* under the same conditions, suggesting that biofoams derived from *L. squarrosulus* were more hydrophobic. This is because biofoams made from *L. squarrosulus* have more uniform fungal skin covering, leading to greater hydrophobicity. In contrast, biofoams made from *P. ostreatus* showed a thin covering of the mycelium filaments on the sample surface, resulting in rough and porous areas. Therefore, it could be inferred that not only the pressing methods and sawdust types can enhance the hydrophobicity of biofoams, but also the physical characteristics of the mycelium, which is characterized by dense coverage and flatness, affect the WCA.

3.3 Cushion Factor

The cushion factor, which is the ratio of the maximum compression stress to the energy density determined by a compression test on biofoams, is presented in Table 4. This dimensionless number can be used to quantify the cushioning performance of the material. In addition, the stress-strain curves of the test provided insights into the mechanical behavior of the biofoams, as shown in Fig. 10. It was found that the biofoams derived from *L. squarrosulus* exhibited nonlinear stress-strain behavior at a strain rate of 0.0085 s^{-1}, which is a typical three-stage behavior of foam materials, with an initial linear elastic region followed by a plateau region and finally densification at higher strains. After the elastic region, the stress increased more slowly with increasing strain, particularly for LS CW-HO and LS CW-CO between strains of 0.1–0.5. At higher strains, the stress began to increase more rapidly, a densification stage occurred, and the internal structure of the biofoam collapsed and compacted. The CW sawdust exhibited the lowest stress levels, indicating the lowest stiffness because of the larger particle size of the sawdust and the higher presence of air voids. In contrast to CC and SW sawdust, the smaller particle size and air voids exhibited the highest stiffness. In terms of pressing methods, HO consistently produced the stiffest biofoams, whereas HP offered the loosest. The biofoam stiffness significantly affects the ability of a material to absorb impact energy [37]. Materials with high stiffness, resulting in high cushion factors, tend to transmit a higher impact force to the product. Materials with low stiffness can deform more under impact, thereby reducing the peak impact force transmitted to the product owing to a low cushion factor.

Table 4: Cushion factor of mycelium-based biofoams compared to EPS foam, PE foam, and corrugated board

Mycelium-based biofoams	Cushion factor
PO CC-HP	6.55 ± 0.21
PO CC-CO	6.64 ± 0.17
PO CC-HO	6.79 ± 0.32
LS CC-HP	5.10 ± 0.19
LS CC-CO	5.26 ± 0.16
LS CC-HO	5.32 ± 0.15
PO SW-HP	6.58 ± 0.26
PO SW-CO	6.67 ± 0.30
PO SW-HO	6.80 ± 0.14
LS SW-HP	4.96 ± 0.19
LS SW-CO	5.06 ± 0.29
LS SW-HO	5.10 ± 0.21
PO CW-HP	6.41 ± 0.15
PO CW-CO	6.43 ± 0.16
PO CW-HO	6.69 ± 0.28
LS CW-HP	4.45 ± 0.16
LS CW-CO	4.65 ± 0.15
LS CW-HO	4.73 ± 0.10
EPS foam	4.00 ± 0.13
PE foam	5.18 ± 0.12
Corrugated board	4.46 ± 0.16

Note: PO: *P. ostreatus*; LS: *L. squarrosulus*; CC: commercial wood sawdust; SW: surface wood sawdust; CW: core wood sawdust, HP: hand-packing, CO: cold pressing, HO: hot pressing.

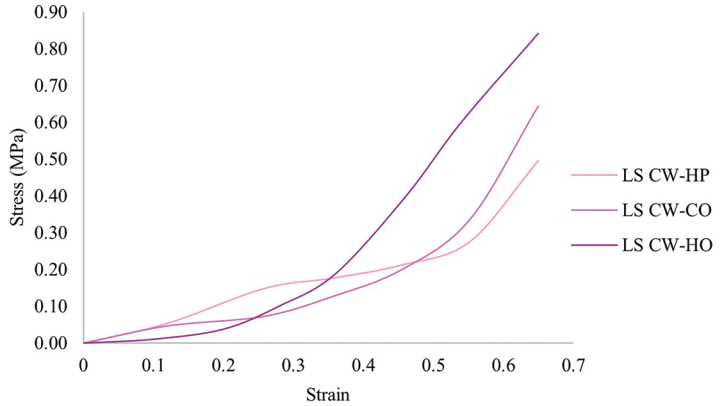

Figure 10: Stress-strain curves of mycelium-based biofoams produced by *L. squarrosulus* (LS) cultivated on CW (core wood sawdust) with hand-packing (HP), cold pressing (CO) and hot pressing (HO) methods at strain rate of 0.0085 s^{-1}

Figure 11: Cushioning factor of mycelium-based biofoams produced by *P. ostreatus* (PO) and *L. squarrosulus* (LS) cultivated on various sawdust types and pressing methods
Note: CC: commercial wood sawdust; SW: surface wood sawdust; CW: core wood sawdust, HP: hand-packing, CO: cold pressing, HO: hot pressing, EPS: expanded polystyrene foam, PE: polyethylene foam.

The results in Table 4 and Fig. 11 show that the combination of mushroom species, sawdust types, and pressing methods significantly influenced the cushion factor of biofoams. *Pleurotus ostreatus* (PO) biofoams generally exhibited higher cushion factors than *Lentinus squarrosulus* (LS) across all studied factors. This suggests that the PO biofoams had a higher dynamic compression stress relative to their energy density, indicating stiffer materials that may not absorb shock as effectively as the LS biofoams. This indicates that LS biofoams have better shock absorption properties due to their cellular structure, which consists of a dense hyphal network with a somewhat uniform distribution on the internal and external surfaces of the biofoams. Furthermore, biofoams cultivated on CW sawdust tend to have lower cushion factors than those cultivated on SW and CC sawdust. Thus, sawdust type significantly affected cushioning performance, with CW sawdust providing a better shock-absorbing material. Moreover, HP consistently offered lower cushion factors than CO and HO pressing methods. This suggests that HO resulted in stiffer biofoams; however, with higher dynamic compression stress, it was not as effective in shock protection. A comparative analysis of the cushion factors for biofoams and traditional packaging materials (EPS foam, PE foam and corrugated board) is essential for evaluating their potential as viable and sustainable alternatives. Only the LS biofoams had cushion factors comparable to those of EPS foam (4.00), corrugated board (4.46), and PE foam (5.18). There were no significant differences among the biofoam cushion factors cultivated on CW sawdust, but there were significant differences compared to the cushion factor of EPS foam. Although biofoams, particularly LS CW-HP, have shown potential, they still face challenges in achieving the same level of cushion factor, uniformity, and structural integrity as EPS foam. EPS foam, a closed-cell structure, the individual cells are isolated from each other, providing a uniform and consistent density throughout the material. The structure contributes to excellent energy absorption and dissipation because the air trapped within these cells acts as a cushion during impact [38]. Conversely, the biofoams exhibited an open cell structure. The cells are interconnected, which can lead to greater variability in cell size and distribution, causing less efficient energy absorption compared to closed-cell structures. The open-cell structure, which is beneficial for biodegradability and environmental

impact, can result in less effective shock absorption, because the interconnected cells collapse more readily under stress. Biofoams can have varying cell sizes, distributions, and densities, depending on the sawdust type and pressing method. Although HP offers the lowest cushion factor, biofoams can suffer from inconsistencies in density and uniformity, leading to uneven performance in cushioning applications owing to the high standard deviation of the cushion factors compared to other pressing methods. To understand the implications of the cushion factor, the thickness of the cushioning materials can be estimated for comparison with EPS foam. According to Eq. (5), if the EPS foam thickness is given as 1 and as the same shock fragility (G) and drop height (h), the thickness of the LS CW-HP biofoam must be 1.11 or 11% thicker in order to achieve shock protection similar to that of EPS foam. Therefore, low cushion factor materials require less material to achieve the desired level of protection.

4 Conclusion

This study demonstrated that the properties of biofoams were significantly influenced by mushroom species, culture media formula, sawdust type, and pressing methods. *Lentinus squarrosulus* (LS) exhibited 32.7% faster growth rate than *Pleurotus ostreatus* (PO), particularly in CW sawdust with bran formula. Biofoams produced from CC and SW sawdust exhibited a more homogeneous and compact structure, which contributed to a 37.7% increase in compression strength and a 15.2% increase in flexural strength compared to biofoams made with CW sawdust. Pressing methods: CO and HO played a crucial role in enhancing the physical and mechanical properties by promoting a denser structure with smaller air voids and a more uniform mycelium distribution. These improvements resulted in a significant increase in density (up to 76.5%), mechanical strength (up to 80% in compression strength and up to 33.3% in flexural strength), and water resistance (up to 54.7% reduction in water absorption). The LS CW-HP biofoam demonstrated superior shock absorption with a cushion factor of 4.45, indicating an 11% increase in cushion thickness compared to the expanded polystyrene (EPS) foam. Despite these advancements, challenges remain in fully matching the shock absorption and other physical characteristics of EPS foam. Future research should explore other agricultural waste substrates, optimize formulations, scale up production, and assess the long-term performance and biodegradability of mycelium-based biofoams under various conditions. Enhancing elasticity through integration with other bio-based materials should also be considered, along with investigating the cushion curves for various densities to support their application in protective packaging. This study provides valuable insights into the potential of mycelium-based biofoams as sustainable alternatives for cushioning materials in packaging applications.

Acknowledgement: The authors thank the Prince of Songkla University and the Faculty of Agro-Industry for equipment and laboratory support.

Funding Statement: This research was supported by the Graduate School, Prince of Songkla University.

Author Contributions: Tanyawan Suwandecha prepared methodology, formal analysis, investigation, original draft. Supachai Pisuchpen supervised and acquired funding, prepared methodology and conceptualization, validated data, reviewed and edited original article. All authors reviewed the results and approved the final version of the manuscript.

Availability of Data and Materials: The datasets generated during the current study will be made available upon request by the corresponding author.

Ethics Approval: Not applicable.

Conflicts of Interest: The authors declare that they have no conflicts of interest to report regarding the present study.

References

1. Lelivelt RR, Lindner GG, Teuffel PP, Lamers HH. The production process and compressive strength of mycelium-based materials. Constr Build Mater. 2015;81:76–82.
2. Rajendran RC. Packaging applications of fungal mycelium-based biodegradable composites. In: Deshmukh SK, Deshpande MV, Sridhar KR, editors. Fungal biopolymer and biocomposites. Singapore: Springer; 2022. p. 275–92. doi:10.1007/978-981-19-1000-5_11.
3. Yang Z, Zhang F, Still B, White M, Amstislavski P. Physical and mechanical properties of fungal mycelium-based biofoam. J Mater Civ Eng. 2017;29(7):04017030. doi:10.1061/(ASCE)MT.1943-5533.0001866.
4. Peng L, Yi J, Yang X, Xie J, Chen C. Development and characterization of mycelium bio-composites by utilization of different agricultural residual byproducts. J Bioresour Bioproducts. 2023;8(1):78–89.
5. Kupradi C, Khongla C, Musika S, Ranok A, Tamaruay K, Woraratphoka J, et al. Cultivation of *Lentinus squarrosulus* and *Pleurotus ostreatus* on cassava bagasse based substrates. Int J Agric Technol. 2017;13(4):883–92.
6. Werghemmi W, Abou Fayssal S, Mazouz H, Hajjaj H, Hajji L. Olive and green tea leaves extract in *Pleurotus ostreatus* var. florida culture media: effect on mycelial linear growth rate, diameter and growth induction index. Earth Environ Sci Trans R Soc Edinb. 2022;1090:012020.
7. Owaid MN, Jaloot AS, Ahmed DM. Influence of *Ficus carica* and *Olea europaea* leaves extracts on the mycelial growth of mushrooms *in vitro*. Acta Ecol Sin. 2018;39(1):36–41. doi:10.1016/j.chnaes.2018.06.003.
8. Elsacker E, Vandelook S, Brancart J, Peeters E, De Laet L. Mechanical, physical and chemical characterisation of mycelium-based composites with different types of lignocellulosic substrates. PLoS One. 2019;14(7):e0213954. doi:10.1371/journal.pone.0213954.
9. Aiduang W, Kumla J, Srinuanpan S, Thamjaree W, Lumyong S, Suwannarach N. Mechanical, physical, and chemical properties of mycelium-based composites produced from various lignocellulosic residues and fungal species. J Fungi. 2022;8(11):1125. doi:10.3390/jof8111125.
10. Kumla J, Suwannarach N, Sujarit K, Penkhrue W, Kakumyan P, Jatuwong K, et al. Cultivation of mushrooms and their lignocellulolytic enzyme production through the utilization of agro-industrial waste. Molecules. 2020;25(12):2811. doi:10.3390/molecules25122811.
11. Zhang W, Ren X, Lei Q, Wang L. Screening and comparison of lignin degradation microbial consortia from wooden antiques. Molecules. 2021;26(10):2862. doi:10.3390/molecules26102862.
12. Joshi K, Meher MK, Poluri KM. Fabrication and characterization of bio-blocks from agricultural waste using fungal mycelium for renewable and sustainable applications. ACS Appl Bio Mater. 2020;3(4):1884–92. doi:10.1021/acsabm.9b01047.
13. Wongjiratthiti A, Yottakot S. Utilisation of local crops as alternative media for fungal growth. Pertanika J Trop Agric Sci. 2017;40(2):295–304.
14. Carlile MJ, Watkinson SC, Gooday GW. Fungal cells and vegetative growth. In: Watkinson SC, Boddy L, Money NP, editors. The fungi. 2nd ed. San Diego, CA, USA: Academic Press; 2001. p. 85–184.
15. Houette T, Maurer C, Niewiarowski R, Gruber P. Growth and mechanical characterization of mycelium-based composites towards future bioremediation and food production in the material manufacturing cycle. Biomimetics. 2022;7(3):103. doi:10.3390/biomimetics7030103.
16. Butu A, Rodino S, Miu B, Butu M. Mycelium-based materials for the ecodesign of bioeconomy. J Nanomater Biostruct. 2020;15(4):1129–40. doi:10.15251/DJNB.2020.154.1129.
17. Appels FV, Camere S, Montalti M, Karana E, Jansen KM, Dijksterhuis J. Fabrication factors influencing mechanical, moisture- and water-related properties of mycelium-based composites. Mater Des. 2019;161:64–71. doi:10.1016/j.matdes.2018.11.027.
18. Powrie WD, Wu CH, Molund VP. Browning reaction systems as sources of mutagens and antimutagens. Environ Health Perspect. 1986;67:47–54.
19. Liu R, Long L, Sheng Y, Xu J, Qiu H, Li X, et al. Preparation of a kind of novel sustainable mycelium/cotton stalk composites and effects of pressing temperature on the properties. Ind Crops Prod. 2019;141:111732.

20. Alemu D, Tafesse M, Deressa YG. Production of Mycoblock from the mycelium of the fungus Pleurotus ostreatus for use as sustainable construction materials. Adv Mater Sci Eng. 2022;2022:1–12. doi:10.1155/2022/2876643.
21. Boadu KB, Nsiah-Asante R, Antwi RT, Obirikorang KA, Anokye R, Ansong M. Influence of the chemical content of sawdust on the levels of important macronutrients and ash composition in Pearl oyster mushroom (*Pleurotus ostreatus*). PLoS One. 2023;18(6):e0287532. doi:10.1371/journal.pone.0287532.
22. Hoa HT, Wang CL. The effects of temperature and nutritional conditions on mycelium growth of two oyster mushrooms (*Pleurotus ostreatus* and *Pleurotus cystidiosus*). Mycobiology. 2015;43(1):14–23.
23. Haneef M, Ceseracciu L, Canale C, Bayer IS, Heredia-Guerrero JA, Athanassiou A. Advanced materials from fungal mycelium: fabrication and tuning of physical properties. Sci Rep. 2017;7(1):41292. doi:10.1038/srep41292.
24. Pena R, Lang C, Naumann A, Polle A. Ectomycorrhizal identification in environmental samples of tree roots by Fourier-transform infrared (FTIR) spectroscopy. Front Plant Sci. 2014;5:229.
25. Galichet A, Sockalingum GD, Belarbi A, Manfait M. FTIR spectroscopic analysis of Saccharomyces cerevisiae cell walls: study of an anomalous strain exhibiting a pink-colored cell phenotype. FEMS Microbiol Lett. 2001;197(2):179–86. doi:10.1111/j.1574-6968.2001.tb10601.x.
26. Schwanninger M, Rodriguez JC, Pereira H, Hinterstoisser B. Effects of short-time vibratory ball milling on the shape of FT-IR spectra of wood and cellulose. Vib Spectrosc. 2004;36(1):23–40. doi:10.1016/j.vibspec.2004.02.003.
27. Manan S, Ullah MW, Ul-Islam M, Atta OM, Yang G. Synthesis and applications of fungal mycelium-based advanced functional materials. J Bioresour Bioproducts. 2021;6(1):1–10.
28. Nava JA, Gonzalez JM, Chacon XR, Luna JAN. Assessment of edible fungi and films bio-based material simulating expanded polystyrene. Mater Manuf Process. 2016;31(9):1085–90. doi:10.1080/10426914.2015.1070420.
29. Ghazvinian A, Farrokhsiar P, Vieira F, Pecchia J, Gursoy B. Mycelium-based bio-composites for architecture: assessing the effects of cultivation factors on compressive strength. Mater Res Innov. 2019;2:505–14. doi:10.5151/proceedings-ecaadesigradi2019_465.
30. Felby C, Hassingboe J, Lund M. Pilot-scale production of fiberboards made by laccase oxidized wood fibers: board properties and evidence for cross-linking of lignin. Enzyme Microb Technol. 2002;31:736–41.
31. Miranda-Valdez IY, Coffeng S, Zhou Y, Viitanen L, Hu X, Jannuzzi L, et al. Foam-formed biocomposites based on cellulose products and lignin. Cellulose. 2023;30(4):2253–66. doi:10.1007/s10570-022-05041-3.
32. Lazo M, Puga I, Macías MA, Barragán A, Manzano P, Rivas A, et al. Mechanical and thermal properties of polyisocyanurate rigid foams reinforced with agricultural waste. Case Stud Chem Environ Eng. 2023;8:100392. doi:10.1016/j.cscee.2023.100392.
33. Namphonsane A, Amornsakchai T, Chia CH, Goh KL, Thanawan S, Wongsagonsup R, et al. Development of biodegradable rigid foams from pineapple field waste. Polymers. 2023;15(13):2895. doi:10.3390/polym15132895.
34. Pędzik M, Auriga R, Kristak L, Antov P, Rogoziński T. Physical and mechanical properties of particleboard produced with addition of walnut (*Juglans regia* L.) wood residues. Materials. 2022;15(4):1280. doi:10.3390/ma15041280.
35. Antinori ME, Ceseracciu L, Mancini G, Heredia-Guerrero JA, Athanassiou A. Fine-tuning of physicochemical properties and growth dynamics of Mycelium-based materials. ACS Appl Bio Mater. 2020;3(3):1044–51.
36. Wessels JGH. Hydrophobins: proteins that change the nature of the fungal surface. Adv Microbial Physiol. 1996;38:1–45. doi:10.1016/S0065-2911(08)60154-X.
37. Tarlochan F. Sandwich structures for energy absorption applications: a review. Materials. 2021;14(16):4731. doi:10.3390/ma14164731.
38. Nechita P, Năstac SM. Overview on foam forming cellulose materials for cushioning packaging applications. Polymers. 2022;14(10):1963. doi:10.3390/polym14101963.